NeuroImage: Clinical 21 (2019) 101654

Contents lists available at ScienceDirect

NeuroImage: Clinical

journal homepage: www.elsevier.com/locate/ynicl

Brain connectivity tracks effects of chemotherapy separately from behavioral measures

Omid Kardan[a,*], Patricia A. Reuter-Lorenz[b], Scott Peltier[b], Nathan W. Churchill[c], Bratislav Misic[d], Mary K. Askren[e], Mi Sook Jung[f], Bernadine Cimprich[b], Marc G. Berman[a,*]

[a] University of Chicago, United States
[b] University of Michigan, United States
[c] St. Michael's Hospital, Canada
[d] Montreal Neurological Institute, Canada
[e] University of Washington, United States
[f] Chungnam National University, South Korea

ARTICLE INFO

Keywords:
Breast cancer
Chemobrain
Functional connectivity
Resting-state BOLD

ABSTRACT

Several studies in cancer research have suggested that cognitive dysfunction following chemotherapy, referred to in lay terms as "chemobrain", is a serious problem. At present, the changes in integrative brain function that underlie such dysfunction remain poorly understood. Recent developments in neuroimaging suggest that patterns of functional connectivity can provide a broadly applicable neuromarker of cognitive performance and other psychometric measures. The current study used multivariate analysis methods to identify patterns of disruption in resting state functional connectivity of the brain due to chemotherapy and the degree to which the disruptions can be linked to behavioral measures of distress and cognitive performance. Sixty two women (22 healthy control, 18 patients treated with adjuvant chemotherapy, and 22 treated without chemotherapy) were evaluated with neurocognitive measures followed by self-report questionnaires and open eyes resting-state fMRI scanning at three time points: diagnosis (M0, pre-adjuvant treatment), 1 month (M1), and 7 months (M7) after treatment. The results indicated deficits in cognitive health of breast cancer patients immediately after chemotherapy that improved over time. This psychological trajectory was paralleled by a disruption and later recovery of resting-state functional connectivity, mostly in the parietal and frontal brain regions. Mediation analysis showed that the functional connectivity alteration pattern is a separable treatment symptom from the decreased cognitive health. Current study indicates that more targeted support for patients should be developed to ameliorate these multi-faceted side effects of chemotherapy treatment on neural functioning and cognitive health.

1. Introduction

Adjuvant chemotherapy is a life-saving procedure in breast cancer treatment. However, considerable evidence suggests that cognitive dysfunction following chemotherapy, referred to in lay terms as "chemobrain," is a serious mental health issue that is poorly understood (Bernstein et al., 2017; Jung et al., 2017; Schagen and Wefel, 2017; Wefel et al., 2011). Recent studies in network neuroscience have shown that relatively sparse patterns of functional connectivity strength during rest can signify broadly applicable neuromarkers of cognitive measures such as sustained attention (Rosenberg et al., 2016) and other psychometric and behavioral measures, thus linking resting state functional connectivity to cognition (e. g., (Biazoli et al., 2017; Smith et al., 2015)). Given the established utility of resting-state neuroimaging in characterizing the neural basis of cognitive (dys)function, we used resting-state Blood-Oxygenation Level Dependent functional Magnetic Resonance Imaging (BOLD fMRI) to investigate changes in functional connectivity pre- to post-treatment and after recuperation, and its relationship with objective and subjective measures of cognitive functioning and health in women diagnosed with breast cancer.

There is ample evidence that chemotherapy is associated with cognitive deficits, and that some deficits are independent of cancer diagnosis and treatment and the accompanying distress (see (Schagen and Wefel, 2017) for a review). However, some studies have linked pre-treatment distress, worry, and fatigue associated with cancer diagnosis and treatment related worry to decreased functional connectivity of the

* Corresponding authors at: 5848 South University Ave, Chicago, IL 60637, United States.
E-mail addresses: okardan@uchicago.edu (O. Kardan), bermanm@uchicago.edu (M.G. Berman).

https://doi.org/10.1016/j.nicl.2019.101654
Received 13 August 2018; Received in revised form 6 December 2018; Accepted 3 January 2019
Available online 06 January 2019

BOLD signal in brain regions associated with attention and memory even before chemotherapy has begun (Andryszak et al., 2017; Churchill et al., 2015; Reuter-Lorenz and Cimprich, 2013). Nevertheless, researchers have yet to identify brain connectivity changes that are due to direct effects of chemotherapy versus connectivity changes that follow the cognitive and emotional distress associated with diagnosis and treatment (Ahles et al., 2010; Askren et al., 2014; Berman et al., 2014a; Cimprich et al., 2010; Dumas et al., 2013; Menning et al., 2015; Wefel et al., 2010). Understanding the brain changes that explain the contribution of overall symptom burden (Jung et al., 2017) to 'chemobrain' is an essential step towards achieving effective interventions before, during, and after chemotherapy in order to more effectively restore cognitive functioning in cancer survivors.

In the current study, we independently controlled the effects of chemotherapy per se by including a group of participants receiving radiation therapy for breast cancer and not chemotherapy (i.e., radiation group). In addition, our study was longitudinal, allowing us to examine changes in brain activity, cognitive performance and subjective performance over one year with time points that coincided with before chemotherapy, one-month after chemotherapy and 7-months later. We examined group by time changes with multivariate analysis methods to identify the pattern of disruption in resting state functional connectivity of the brain due to overall cancer treatment as well as chemotherapy vs. non-chemotherapy (controlling for having cancer) and the degree to which those patterns of disruption can be linked to measures of distress and cognitive performance. Here we quantify: 1) the effect of chemotherapy on resting-state functional connectivity, 2) the effect of chemotherapy on objective and subjective measures of cognitive performance and well-being, and 3) the relationship between resting-state functional connectivity and objective and subjective psychological measures as they track the chemotherapy effects. These results will have important implications for how to treat the psychological and physiological effects on the brain that accompany breast cancer treatment and improve patients' recovery from a psychological and physiological standpoint.

2. Methods

2.1. Participants

Sixty six right-handed women were recruited for 3 sessions from the University of Michigan Comprehensive Cancer Center, including two groups of women surgically treated for breast cancer (stage 0 – IIIa, see Table 1) awaiting adjuvant chemotherapy (CT, $n = 22$) or radiation-therapy without chemotherapy (non-CT, n = 22) and age-matched healthy controls (HC, n = 22) with negative mammograms that occurred within a year. The present study's sample of 66 is the subset of 92 women in Jung et al., (2017) who received resting state fMRI. Four women of the CT group did not return for post-baseline assessments due to unstable medical conditions or new MRI contraindications, resulting in $n = 18$ patients from the CT group to have data for all 3 time points. Screening criteria included absence of cognitive disorder (Mini-Mental Status Examination) (Folstein et al., 1975), clinical depression (Patient Health Questionnaire, PHQ-8) (Kroenke et al., 2009), and secondary diagnosis of neurological or psychiatric disorders. The University of Michigan Institutional Review Board for Medicine approved all the studies, and all participants provided written informed consent.

2.2. Design

Participants were evaluated with neurocognitive measures followed by self-report questionnaires and open eyes resting-state fMRI scanning at three time points. Assessments occurred at: diagnosis (M0, pre-adjuvant treatment), at least 1 month (M1), and 7 months (M7) after completion of treatment, resulting in 186 completed fMRI scanning sessions.

Table 1
Sample characteristics.

Characteristics	CT (n = 18)		Non-CT (n = 22)		HC (n = 22)	
	n (%)	Mean (SD)	n (%)	Mean (SD)	n (%)	Mean (SD)
Age (year)		49.22 (11.13)		53.82 (8.18)		51.13 (8.79)
Education (year)		15.17 (2.38)		15.05 (2.15)		16.54 (1.84)
Race[a]						
White	14 (78)		19 (86)		20 (91)	
Non-white	4 (22)		3 (14)		2 (9)	
Stage						
0	0 (0)		9 (41)		–	
I	4 (22)		11 (50)		–	
II	10 (56)		2 (9)		–	
IIIa	4 (22)		0 (0)		–	
Hemoglobin (g/dl)						
M0		12.51 (0.72)		13.63 (0.70)		13.12 (0.92)
M5		12.14 (0.89)		13.17 (0.79)		13.17 (0.84)
M12		12.91 (0.75)		13.70 (0.82)		13.21 (1.08)

Abbreviations: CT, chemotherapy-treated; non-CT, treated without chemotherapy; HC, healthy control; M0, baseline; M5, five-month follow-up; M12, twelve-month follow-up.

[a] 85% Caucasian, 8% African American, 5% Asian American, 2% Native American.

2.3. Self-reported measures and objective tasks

Cognitive health of the participants was measured using objective cognitive performance and subjective emotional and cognitive well-being measures (i. e., behavioral variables). Subjective assessments included cognitive complaints (Attentional Function Index, AFI), physical symptom severity (Breast Cancer Prevention Trial symptom scales, BCPT) (Cella et al., 2008), psychological distress- worry (Three-Item Worry Index, TIWI) (Kelly, 2004), anxiety (State-Trait Anxiety Inventory, STAI) (Spielberger Charles, 2010), depression (PHQ-8) (Kroenke et al., 2009), fatigue (Functional Assessment of Cancer Therapy: Fatigue, FACT-F) (Yellen et al., 1997), and sleep problems (Pittsburgh Sleep Quality Index, PSQI) (Buysse et al., 1989).

Objective cognitive assessments included the Verbal Working Memory Task (VWMT) that occurred during a separate fMRI scanning (Askren et al., 2014; Berman et al., 2014a; Nelson et al., 2003), and two Digit Span tasks: Backwards (DSB) and Forward (DSF) (Gerton et al., 2004; Reynolds, 1997). For each trial (total of 192) in the VWMT, participants were presented with a set of four letters for 1500 ms. Following a 3000 ms delay interval, they were presented with a "probe" letter for 1500 ms and asked whether it was a member of the current memory set. This task was done during four runs of fMRI scanning for which the brain data were reported in a previous study (Jung et al., 2017). For the current study we used the reaction time (RT) and accuracy measures of the VWMT.

2.4. fMRI acquisition parameters

Images were acquired on a GE SIGNA 3 Tesla scanner, equipped with a standard quadrature head coil. Functional T2* weighted images were acquired using a spiral sequence with 25 contiguous slices with 3.75 × 3.75 × 5 mm voxels with repetition time (TR) = 1500 ms; echo time (TE) = 30 ms; flip angle =70°; field of view (FOV) = 24 cm for 360 s of rest (eyes open). A T1-weighted gradient echo anatomical overlay was acquired using the same FOV and slices (TR = 225 ms, TE = 5.7 ms, flip angle = 90°). Additionally, a 124-slice high-resolution T1- weighted anatomical image was collected using spoiled gradient-

recalled acquisition in steady-state imaging (TR = 5 ms, TE = 1.8 ms, flip angle = 15, FOV = 25–26 cm, slice thickness = 1.2 mm).

2.5. fMRI preprocessing

We used the Optimization of Preprocessing Pipelines for NeuroImaging software (OPPNI, (Churchill et al., 2011; Churchill et al., 2012)) which perform automated processing and quality assessment of the fMRI data, using a combination of freeware packages from AFNI (https://afni.nimh.nih.gov) and FSL (https://www.fmrib.ox.ac.uk/fsl) along with custom algorithms. Processing included rigid-body motion correction (AFNI *3dvolreg*), slice-timing correction (AFNI *3dTshift*), spatial smoothing with 6 mm FWHM Gaussian kernel (AFNI *3dmerge*), along with motion parameter regression (regressing out motion PCs that account for > 85% of head movement parameters variance) and temporal detrending (Legendre polynomials of order 0 to 4) on the resting-state time-series. The data-driven PHYCAA+ algorithm (Churchill and Strother, 2013) was used to estimate and remove physiological noise components. We used a linear filter to suppress BOLD frequencies above 0.10 Hz. Finally, spatial normalization to group template was performed as follows: FSL *flirt* was used to compute the rigid-body transform of the mean functional volume for each participant in a session to their T1-weighted anatomical scan, along with the 12-parameter affine transformation of the T1 image for the participant to the MNI152 template. The transformation matrices were then concatenated, and the net transform applied to the fMRI data. The preprocessing of high-resolution T1- weighted anatomical images included removing the non-brain tissue and skull using the brain extraction tool (FSL *bet*), down sampling the images to the MNI152 template resolution, and normalizing them to the MNI152 template.

2.6. Statistical analysis

Contrast Partial Least Squares (PLS; (Krishnan et al., 2011; McIntosh and Lobaugh, 2004)) analysis was used to identify the relationship between the set of behavioral variables organized as group-by-time blocks (results section 1), as well as the functional connectivity of the segmented brain regions from the whole brain with the group-by-time blocks (results section 2). To reduce the number of possible connections in the entire voxel space, i. e., $C(102{,}400, 2) = 5*10^9$, the whole brain for each subject was first segmented into 116 regions based on the Automated Anatomical Labeling (AAL) atlas (Tzourio-Mazoyer et al., 2002). This was done by normalizing the AAL atlas to the MNI152 and averaging the voxels of the normalized T2* weighted images within each AAL region for each participant. The connectivity matrix is then calculated (Pearson correlations) for these parcellated data. This yields $C(116, 2) = 6670$ unique pairwise connections between AAL regions shown in Fig. 1A as the sub-diagonal elements of the 116*116 correlation matrix for each subject at each time point. The PLS technique allows for identification of significant relationships between two sets of variables (for example functional connectivity values and treatment levels in the study, e. g. see (Berman et al., 2014b; Cloutier et al., 2017)) in a data-driven manner. The PLS implementation software was downloaded from Randy McIntosh's lab at: https://www.rotman-baycrest.on.ca/index.php?section=84. The version of PLS that we implemented was created on 05-JAN-2005 by Jimmy Shen and updated as part of Pls.zip: 16-MAY-2012.

In PLS, the goal of the analysis is to find weighted patterns of the original variables in the two sets (termed “latent variables” or “LVs”) that maximally co-vary with one another. In contrast PLS, these LVs represent a differentiation between levels of experimental design (i. e., three timepoints: pre-treatment, 1 month, and 7 months post-treatment and three groups: chemotherapy, non-chemotherapy breast cancer, and aged-matched healthy controls in this study) interpreted as a contrast with 3*3 = 9 levels, as well as a spatial pattern of voxel activity that supports that contrast (in the case when the other set of variables is BOLD timeseries) or a weighted sum of the behavioral variables (when the other set of variables is behavioral variables). In the current study there are a total of 186 brain measurements, as well as 186 measurements for every behavioral variable (3 times for each participant in each group). These 186 measures are averaged across groups and time to create the X matrix, yielding an X of size 9 * 6670 and 9*11 for brain connections and behavioral variables, respectively. The Y matrix is the 9*9 experimental design matrix contrasting groups and times. PLS is computed via singular value decomposition (SVD; (Eckart and Young, 1936)). The covariance between the two data sets X (e.g. mean-centered[1] brain matrix of size 9 × 6670 connections or z-scored behavioral matrix of size 9 × 11 behavioral variables) and Y (e.g. experimental design matrix of size 9 × 9 group-by-time contrasts) is computed (X'Y) and is subjected to the SVD:

$$SVD(X'Y) = USV'$$

Resulting in a set of orthonormal matrices U and V (termed left and right singular vectors, respectively), as well as a diagonal matrix S of singular values. The number of LVs from the analysis is equal to the smallest rank of its constituent matrices (the rank of the covariance matrix X'Y, which is equal to 9, the degrees of freedom in the experimental design in the current study). The *i*th LV is comprised of a triplet of *i*th left singular vector, the *i*th right singular vector, and the *i*th singular value. The right and left singular vectors provide weights (or “saliences”) for the two sets (behavioral variables and treatment levels or voxels and treatment levels), respectively. The scalar singular value is proportional to the “crossblock covariance” between X and Y captured by the LV, and is naturally interpreted as the effect size of this statistical association.

The LVs are linear combinations of behavioral variables or voxel activities across the whole brain whose combinations are differentially instantiated for different groups * time cells. In other words, the left singular vector in the current study contains the weights for levels in the groups * times set and the right singular vector contains the loadings for behavioral measures (Results section 1) or saliences of connectivity between brain regions (Results section 2). Multivariate methods applied to fMRI data offer a novel opportunity to discover meaningful associations between distributed patterns of brain activities and experimental conditions in a single statistical model, as opposed to univariate methods where conditions are regressed on every voxel or cluster of voxels separately. To test the significance of each LV, a set of 1000 covariance matrices were generated by randomly permuting condition labels for the X variables (brain or behavioral measures set). These covariance matrices embody the null hypothesis that there is no relationship between X and Y variables. They were subjected to SVD as before resulting in a null distribution of singular values. The significance of the original LV was assessed with respect to this null distribution. The *P* value was estimated as the proportion of the permuted singular values that exceed the original singular value.

The reliability with which each functional connection or behavioral variable contributes to the overall multivariate pattern was determined with bootstrapping. A set of 1000 bootstrap samples were created by resampling subjects with replacement within each group*time cell (i.e. preserving condition labels). Each new covariance matrix was subjected to SVD as before, and the singular vector weights from the resampled data were used to build a sampling distribution of the saliences from the original data set. The purpose of a constructed bootstrapped sampling distribution is to determine the reliability of each salience (i.e. saliences that are highly dependent on which participants are included in the analysis will have wide distributions).

For the brain connections, a single index of reliability (termed “bootstrap” ratio, or “Z_{BR}”) was calculated by taking the ratio of the

[1] The mean-centering is done on group level to remove the group-mean differences and maximize sensitivity to treatments (intra-group time effects).

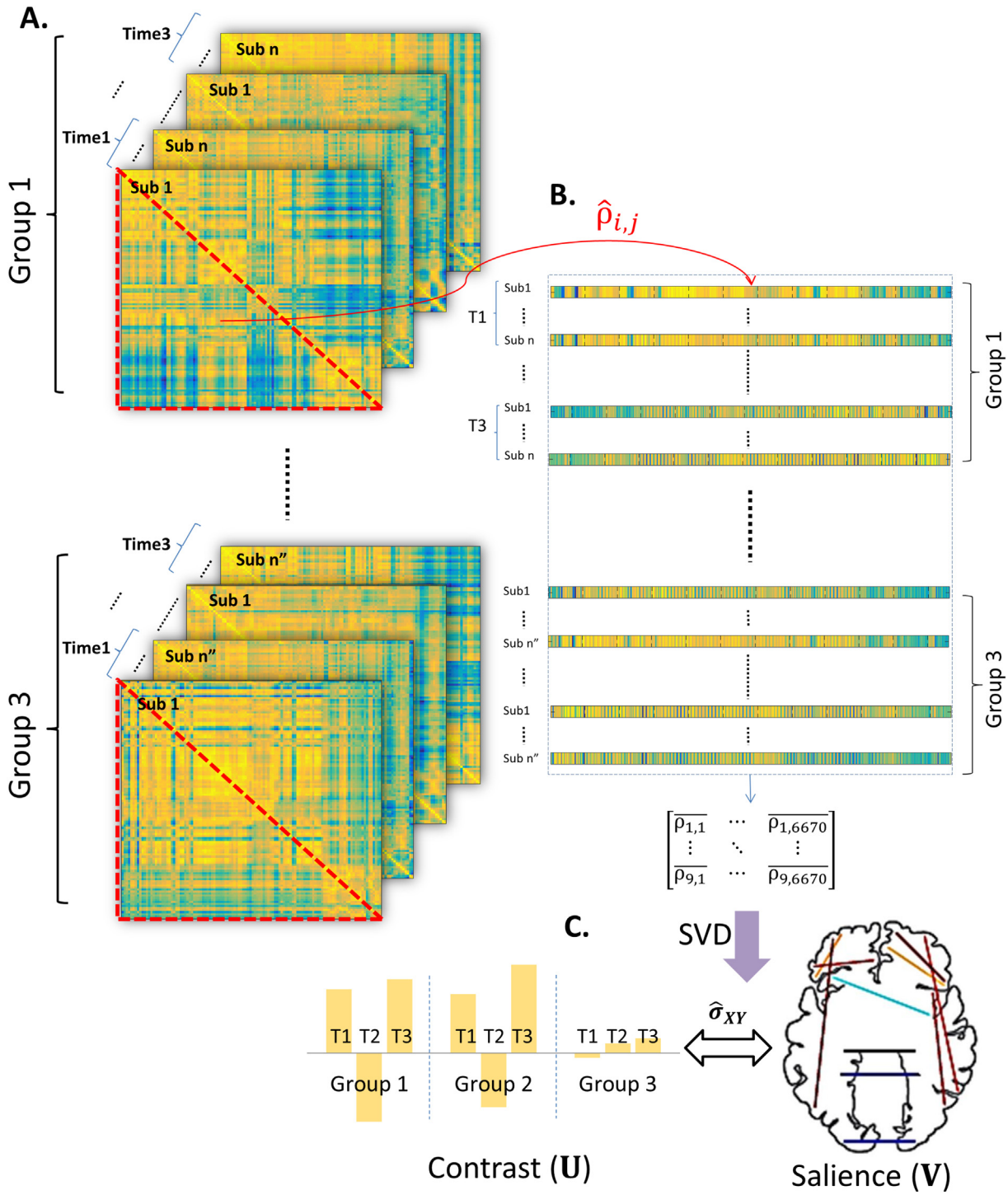

Fig. 1. Schematic of contrast PLS for the brain data. A. Functional connectivity matrices: To reduce the number of possible connections in the all voxels space, i. e., C(102,400, 2) = 5*10^9, the whole brain for each subject was first segmented into 116 regions based on the Automated Anatomical Labeling (AAL) atlas (Tzourio-Mazoyer et al., 2002). This yields C(116, 2) = 6670 connections between AAL regions shown as a symmetric 116*116 correlation matrix for each subject at each time. B. The elements below main diagonal of connectivity matrices ($\hat{\rho}_{i,j}$ shows the Pearson correlation between BOLD time-series of two regions) are reshaped into a one-dimensional vector of size 1*6670 and stacked with the other participants within the same time, and then nested within the group. Then, the resulting matrix that contains all functional connectomes of all subjects averaged across times and groups and procedures described in the methods involving Singular Value Decomposition is applied to it. C. The resulting left singular vector (U, experimental conditions contrast) and right singular vector (V, brain connectivity salience) are shown, with the proportion of total covariance the LV is accounting for (Cross-block $\hat{\sigma}_{XY}$) calculated as its squared singular value divided by sum of squares of singular values in the S matrix. The confidence intervals for loadings and bootstrap ratios for saliences are calculated using non-parametric (re-sampling) procedures described in the methods.

salience to its bootstrap estimated standard error. A Z_{BR} for a given connection is large when the connection has a large salience (i.e. makes a strong contribution to the LV) and when the bootstrap estimated standard error is small (i.e. the salience is stable across many resamplings). Here, connections with $Z_{BR} > 3$ or $Z_{BR} < -3$ were selected as showing reliable increase or decrease in functional connectivity,

respectively (equivalent to p~0.0025, 2-tailed, under normal distribution assumptions). The process of applying PLS to relate the resting-state functional connectivity matrices to the group*time contrast is described in Fig. 1.

The process of applying PLS to the behavioral variables with the group*time contrast is similar, except that the matrix fed into the SVD contains the behavioral values instead of correlations between BOLD response of different brain regions. This would mean that each row vector for a participant at a timepoint is their 1*11 behavioral vector instead of 1*6670 connectivity vector. These row vectors are then stacked to create the behavioral matrix that will be used in the SVD (equivalent to the stacked connectivity matrix shown in Fig. 1 section B).

2.7. Mediation analysis

The mediations were implemented using R package 'mediation' (Tingley et al., 2014) with quasi-Bayesian confidence intervals. The functional connectivity pattern associated with treatment and recovery was first aggregated for each participant at each scanning session. Because all the saliences are positive in the LV, this aggregation was done simply by summing up the Fisher's z-transformed correlations between the regions that showed reliable connectivity change (i. e., the parietal-frontal connections with $Z_{BR} > 3$ from Fig. 3). Alternatively, brain data from each subject can be projected on the singular vectors to get one aggregated score for the 214 saliences for each subject. The two methods yielded very similar results with aggregated measures from the two methods being correlated with r = 0.944, Pearson correlation. Hence, we are reporting the aggregated measure based on the first method described above as it is more intuitive. For simplicity, this will be referred to as the Aggregated Parieto-Frontal (APF) connectivity.

3. Results

As the mean-centering of the behavioral variables and functional connectivity values in the PLS were done at the group-mean level, the results presented in the following sections only include intra-group differences considering time effects. This ensures sensitivity to the treatment effects as the focus of the study is the pre- to post- chemotherapy and recuperation effects on women diagnosed with breast cancer.

3.1. Behavioral results

We examined the primary treatment contrast (M0, M1, and M7 by CT, nonCT, and HC), i.e., the one that covaried maximally with the behavioral measures, using the Partial Least Squares (PLS) multivariate analysis procedure (see Methods: *Statistical Analysis*; For simple statistics of behavioral measures across groups and time points please see supplementary Table S1.). This latent variable is shown in Fig. 2, the subsequent LVs did not pass the permutation null threshold of $p < .01$ and will not be discussed further. The Cross-block covariance between this emerged experimental condition contrast (Fig. 2, top) and cognitive health measures (Fig. 2, bottom) is relatively large ($\hat{\sigma}_{XY} = 0.48$), showing that the behavioral variables we measured as indicators of cognitive health can notably signify the status change of the patients pre-to post-treatment and recuperation.

The results show that the CT group at M1 is strongly affected by their treatment as exhibited in that group having more fatigue, depression, and physical burdens (BCPT), as well as lower self-reported attention (AFI) and lower performance on digit spans (DSB and DSF) compared to their baseline state at M0 (indicated by red line in Fig. 2 top panel), and recovery state at M7 (indicated by green line in Fig. 2 top panel). This decrease in objective cognitive performance and subjective emotional and cognitive well-being (henceforth referred to as decrease in cognitive health) at M1 compared to M0 and M7 is much smaller for the non-CT group and not present for the HC group. Therefore, we will be referring to this latent variable as chemotherapy treatment's effect (detrimental effect M0 to M1, red) plus recuperation's effect (beneficial effect M1 to M7, green) on cognitive health.

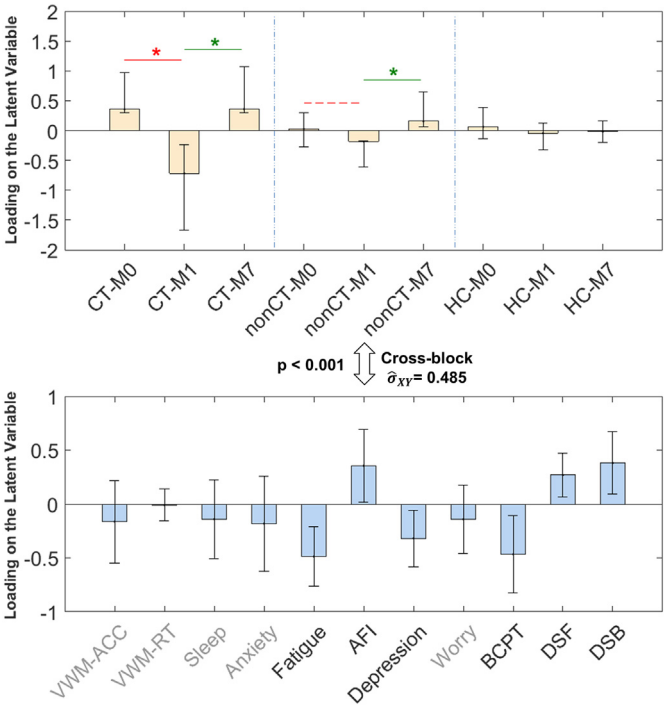

Fig. 2. PLS results (LV1) relating experimental conditions (group * time, top panel) to the behavioral measures (bottom panel). Errorbars show 95% confidence intervals as indicated by bootstrapping. Cross-block covariance $\hat{\sigma}_{XY}$ shows the cross-covariance between the two sets of data. The magnitude of loading for each variable shows its contribution to the LV. The red line with * indicates statistically significant ($p < .001$) treatment effect between M1 and M0 for the CT group. The green lines with * indicate significant ($p < .001$) recuperation effects between M1 and M7 for CT and non-CT groups. Grayed-out variable names show non-significant loading ($p > .05$) for the behavioral variable in the LV.

3.2. Resting-state functional connectivity results

Next, PLS was used to find the optimum treatment contrast that maximally covaried with changes in functional connectivity between brain regions (see Methods). Here, again, the first latent variable is the only one that passed the permutation null threshold of $p < .01$ and therefore the subsequent LVs will not be discussed further.

The results, shown in Fig. 3, indicate a relatively distributed pattern of functional connectivity mostly in parietal and frontal regions of the brain that decreases in connectivity strength at M1 compared to M0 and then increases again at M7 for patient groups (especially the CT group). There are 214 reliable connections in the pattern ($Z_{BR} > 3$) which includes ~3% of all the possible connections (See *Supplementary Results* Figs. S1 and S2 for the list of anatomical labels of the connections). Importantly, the emerged group-by-time contrast resembles the one previously found for behavioral measures (although not identical), hence we will refer to this latent variable as chemo treatment plus recuperation's effects on functional connectivity. To emphasize the similarity between this LV and the one regarding cognitive health from the previous analysis, we again indicated the M0 to M1 contrast by red and the M1 to M7 contrast by green lines in Fig. 3, respectively.

The proportion of covariance accounted for by this LV is also similar to that of the cognitive health measures (Cross-block $\hat{\sigma}_{XY} = 0.53$ compared to 0.48 from the behavioral LV) which shows that this

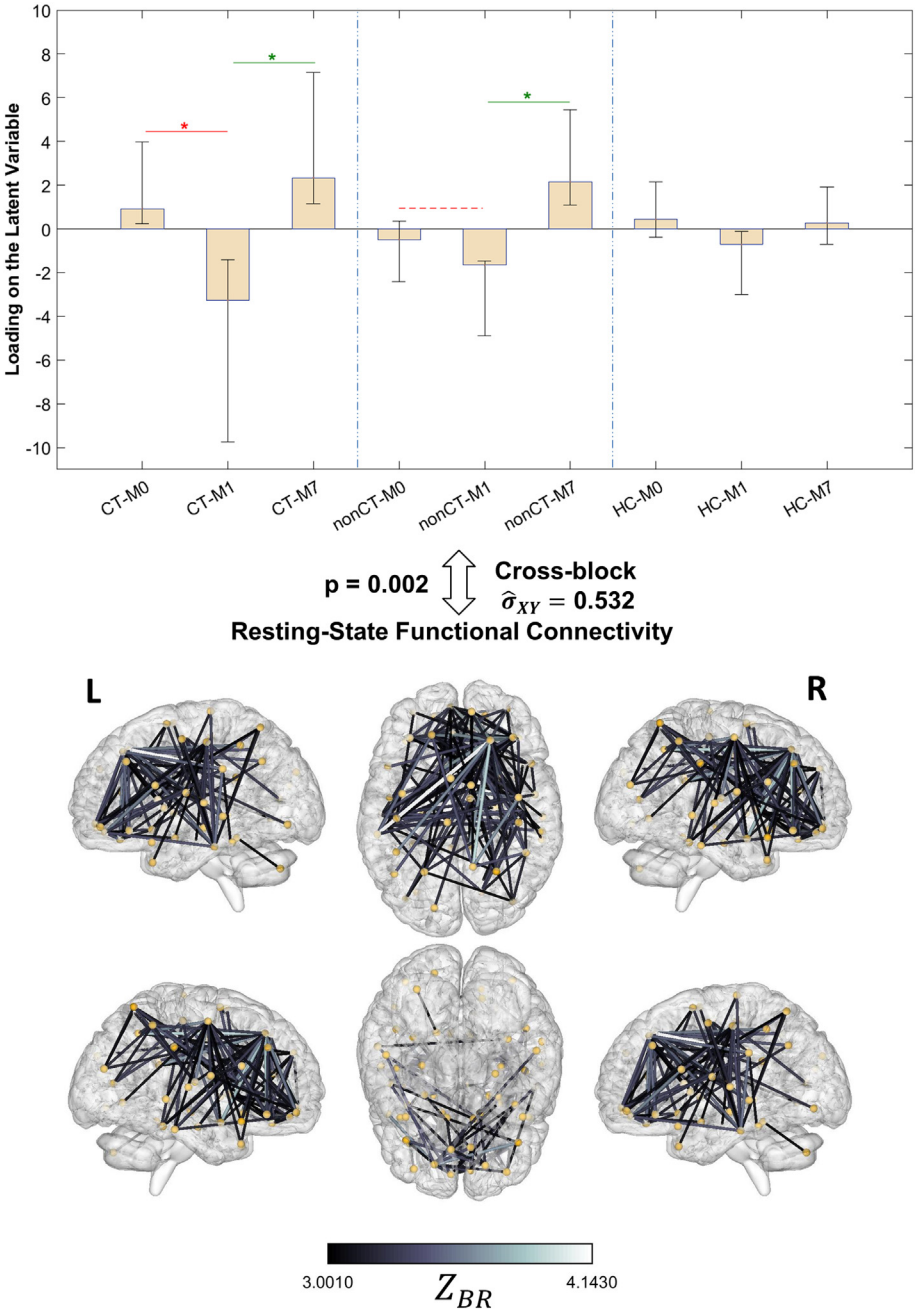

Fig. 3. PLS results (LV1) relating experimental conditions (group * time, top panel) to brain functional connectivity (bottom panel). Errorbars show 95% confidence intervals as indicated by bootstrapping. Cross-block $\hat{\sigma}_{XY}$ shows the proportion of covariance between the two sets explained by this LV. All edges in bottom panel show connections with Bootstrap ratio Z_{BR} values above 3 indicating reliable increase in connectivity strength, with lighter colors having greater Z_{BR} values. There were no connections with $Z_{BR} < -3$, indicating lack of any connections that reliably decreased for this latent variable. The red line with * in the top panel indicates a statistically significant ($p < .001$) treatment effect between M1 and M0 for the CT group. The green lines with * in the top panel indicate significant ($p < .001$) recuperation effects between M1 and M7 for CT and non-CT groups.

resting-state functional connectivity pattern could potentially be a neural signal that is as consistent as the cognitive health measures in capturing the effects of cancer treatment (especially chemotherapy) and recovery on patients.

3.3. Relationship between cognitive health and functional connectivity measures

The similarity between the experimental conditions (time-by-group) LVs resulting from the two previous analyses (top panels in Figs. 2 and 3, r = 0.903, Pearson correlation between primary right singular vectors in the two PLS analyses) suggests a potential relationship between the parieto-frontal functional connectivity pattern found in the brain connectivity LV (Fig. 3 bottom panel) and the dip in cognitive health evident in the behavioral LV (Fig. 2 bottom panel, i. e., more fatigue, depression, BCPT, lower AFI, DSB and DSF). In other words, both LVs could reflect the same phenomenon but in different domains (BOLD vs. behavior). Statistical evidence for this "common cause" hypothesis requires that shared covariance between the brain connectivity and experimental conditions overlaps with the shared covariance between the behavioral measures and experimental conditions.

To test this possibility, we first calculated an aggregated parieto-

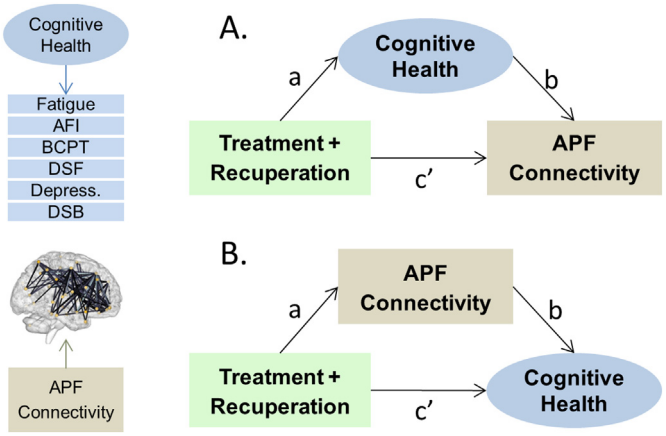

Fig. 4. Two alternative causal mediation models. The panel on the left shows the constituent variables for cognitive health (top) and Aggregated Parieto-Frontal connectivity (bottom) latent variables, respectively. Treatment + Recuperation is simple contrast coding of M1 vs. M0 and M7 for patient groups. A. Model used for testing if the chemotherapy + recuperation effects on functional connectivity in the parieto-frontal connectome is (partially) mediated by the cognitive health of the patients. B. Model used for testing if the chemotherapy + recuperation effects on cognitive health of the patients is (partially) mediated by functional connectivity in the parieto-frontal connectome. For both models the a*b path shows the mediated effect and the c′ path is the direct effect.

frontal (APF) measure of the functional connectivity pattern for each subject (see methods: *Mediation Analysis*). Next, we tested two alternative causal mediation models (Fig. 4) to assess A) whether the APF connectivity disruption occurs, at least partially, as a result of cognitive health deficits (i. e., the LV consisted of higher fatigue, depression, BCPT, and lower AFI, DSB, and DSF), or alternatively B) whether the cognitive health deficits are partially caused by the APF connectivity disruption.

The results of the mediation analyses showed no evidence for either cognitive health mediating the chemotherapy treatment's effect on APF connectivity (Model A: a*b = 0.01, Quasi Bayesian 95% CI = [−0.07, 0.08], p = .93) or the APF connectivity mediating the effect of chemotherapy on cognitive health (Model B: a*b = 0.02, Quasi Bayesian 95% CI = [−0.14, 0.16], p = .82). However, the direct effect of chemotherapy treatment + recuperation (c′) is significant in predicting both APF connectivity (Model A: c′ = 0.56, Quasi Bayesian 95% CI = [0.19, 0.91], p < .01) and cognitive health (Model B: c′ = 0.79, Quasi Bayesian 95% CI = [0.18, 1.41], p < .01) in both models. This implies that two different aspects of the chemotherapy process are responsible for the decrease in functional connectivity in the parietal-frontal connectome and increased distress and cognitive complaints after treatment.

4. Discussion

In the current study, we first showed a deterioration in measures of cognitive and emotional well-being of breast cancer patients immediately after chemotherapy that they subsequently recovered from by 7 months after treatment. Specifically, the chemotherapy patients reported more fatigue, depression, physical burdens (BCPT), and poorer attentional function (AFI), and performed worse on objective cognitive tasks (DSB and DSF) compared to their state before adjuvant therapy and 7 months after therapy. These results are in line with dynamics of some of the cognitive decline measures previously reported (Andryszak et al., 2017; Menning et al., 2015). Parallel to this cognitive health deficit and recovery, we found an extensive, unidirectional change (decrease) in brain connectivity of the patients, where resting-state BOLD functional connectivity in parietal and frontal brain regions was disrupted as an apparent result of treatment (much stronger with chemotherapy but also present for non-chemotherapy treatments such as radiation therapy). These results complemented the previous studies on functional connectivity of the brain after chemotherapy from more limited longitudinal and group-level designs (Bernstein et al., 2017; Bromis et al., 2017; Dumas et al., 2013). Finding a single significant (high-variance) latent variable from the PLS analyses in the brain connectivity and behavior domains, as opposed to multiple significant non-primary LVs in each domain, indicates a robust response pattern across individuals in a single network of brain areas and a single set of behavioral variables, respectively.

Interestingly, similar to the cognitive health deficits, the functional connectivity disruption pattern also abates by 7 months. Despite the similarity in the longitudinal dynamics of the behavioral changes and the brain connectivity disruptions, the latter seems to emerge as a chemotherapy treatment symptom separate from the cognitive health deficits (i. e., neither caused by them nor causing them in a statistically significant manner as indicated by the results of our two mediation models). It is possible that these resting-state results reflect more basic physiological changes that may be challenging to measure with self-report psychological tests and too subtle for the objective cognitive tasks (for example see Castellon et al. (2004); Ferguson et al. (2007)). Our measurements of cognitive health cover a comprehensive spectrum of cognitive performance and emotional health. Admittedly, however, there could be other dimensions of cognitive functioning tied to prefrontal and posterior parietal cortices that the current study did not measure (such as complex decision making, reasoning, rumination, etc.) and are affected by the connectivity disruption reported here (or are responsible for the disruptions). Further research is required to pinpoint the mechanism through which chemotherapy is resulting in decreased resting-state BOLD connectivity. Until then, interventions aiming to improve the quality of life for cancer patients need to be directed towards improving behavioral performance and self-perceived well-being of the patient, especially during the first month after adjuvant chemotherapy (Fawzy et al., 1995; Swainston and Derakshan, 2018).

The current study's results imply that clinicians and medical professionals can utilize and apply resting-state functional connectivity in clinical populations more broadly and as a source of non-redundant information about patients, as it serves a complementary signal to the psychometric measures. While resting state functional connectivity has previously been used in clinical research and assessment of patient status (see for example Fox and Greicius (2010); Greicius (2008)), there are limited studies that directly compare its predictive power to that of more convenient 'pencil and paper' behavioral variables in clinical populations (Iordan et al., 2018; Kaiser et al., 2015). We hope that these results help to motivate more inquiry about potential applications of resting-state functional connectivity signals to investigate side effects of intrusive, but life-saving, treatment procedures on brain function of clinical populations.

In conclusion, we have shown that resting-state functional connectivity in regions mostly within parieto-frontal network follows along the treatment and recovery dynamics of breast cancer treatment and recovery and explains as much variance in these treatment dynamics as a battery of behavioral self-report and objective measures of cognitive and physical well-being. We also demonstrated that this parieto-frontal resting state functional connectivity disruption fails to be proposed as a mechanistic explanation of the changes in cognitive well-being and the behavioral cognitive dysfunction of chemo patients. Interestingly and importantly, each measure explains unique variance in treatment dynamics. It will be important to understand what aspects of treatment and recovery are captured by the resting-state functional connectivity and what psychological factors are in fact related to it. More targeted support should be devoted to understanding how to ameliorate the multifaceted side effects of cancer treatment and the 'chemo-brain'.

Author contributions

MGB, PRL, and BC devised the study design. PRL, MJ, MKA, BC, SP, and MGB collected the fMRI and behavioral data. OK, MGB, NWC, and BM analyzed the data and OK made the figs. OK wrote the first draft of the manuscript and all authors critically contributed to the final version of the manuscript.

Competing interests

The authors declare no competing interests.

Acknowledgements

This work was supported in part by NIH grant (NIH-NINR-R01-NRO10939) to BC, a TKF foundation grant, Templeton Grant ID#: 37775 from the John Templeton Foundation (www.templeton.org) and a National Science Foundation (NSF) grant #1632445 to MGB.

Appendix A. Supplementary data

Supplementary data to this article can be found online at https://doi.org/10.1016/j.nicl.2019.101654.

References

Ahles, T.A., Saykin, A.J., McDonald, B.C., Li, Y., Furstenberg, C.T., Hanscom, B.S., Mulrooney, T.J., Schwartz, G.N., Kaufman, P.A., 2010. Longitudinal assessment of cognitive changes associated with adjuvant treatment for breast cancer: impact of age and cognitive reserve. J. Clin. Oncol. 28, 4434–4440. https://doi.org/10.1200/JCO.2009.27.0827.

Andryszak, P., Wiłkość, M., Izdebski, P., Żurawski, B., 2017. A systemic literature review of neuroimaging studies in women with breast cancer treated with adjuvant chemotherapy. Contemp. Oncol. (Pozn) 21, 6–15. https://doi.org/10.5114/wo.2017.66652.

Askren, M.K., Jung, M., Berman, M.G., Zhang, M., Therrien, B., Peltier, S., Ossher, L., Hayes, D.F., Reuter-Lorenz, P.A., Cimprich, B., 2014. Neuromarkers of fatigue and cognitive complaints following chemotherapy for breast cancer: a prospective fMRI investigation. Breast Cancer Res. Treat. 147, 445–455. https://doi.org/10.1007/s10549-014-3092-6.

Berman, M.G., Askren, M.K., Jung, M., Therrien, B., Peltier, S., Noll, D.C., Zhang, M., Ossher, L., Hayes, D.F., Reuter-Lorenz, P.A., Cimprich, B., 2014a. Pretreatment worry and neurocognitive responses in women with breast cancer. Health Psychol. 33, 222–231. https://doi.org/10.1037/a0033425.

Berman, M.G., Misic, B., Buschkuehl, M., Kross, E., Deldin, P.J., Peltier, S., Churchill, N.W., Jaeggi, S.M., Vakorin, V., McIntosh, A.R., Jonides, J., 2014b. Does resting-state connectivity reflect depressive rumination? A tale of two analyses. NeuroImage 103, 267–279. https://doi.org/10.1016/j.neuroimage.2014.09.027.

Bernstein, L.J., McCreath, G.A., Komeylian, Z., Rich, J.B., 2017. Cognitive impairment in breast cancer survivors treated with chemotherapy depends on control group type and cognitive domains assessed: a multilevel meta-analysis. Neurosci. Biobehav. Rev. 83, 417–428. https://doi.org/10.1016/j.neubiorev.2017.10.028.

Biazoli, C.E.J., Salum, G.A., Pan, P.M., Zugman, A., Amaro, E.J., Rohde, L.A., Miguel, E.C., Jackowski, A.P., Bressan, R.A., Sato, J.R., 2017. Commentary: Functional connectome fingerprint: identifying individuals using patterns of brain connectivity. Front. Hum. Neurosci. 11. https://doi.org/10.3389/fnhum.2017.00047.

Bromis, K., Gkiatis, K., Karanasiou, I., Matsopoulos, G., Karavasilis, E., Papathanasiou, M., Efstathopoulos, E., Kelekis, N., Kouloulias, V., 2017. Altered brain functional connectivity in small-cell lung cancer patients after chemotherapy treatment: a resting-state fMRI study [WWW Document]. Comp. Math. Method. Med. https://doi.org/10.1155/2017/1403940.

Buysse, D.J., Reynolds, C.F., Monk, T.H., Berman, S.R., Kupfer, D.J., 1989. The Pittsburgh sleep quality index: a new instrument for psychiatric practice and research. Psychiatry Res. 28, 193–213. https://doi.org/10.1016/0165-1781(89)90047-4.

Castellon, S.A., Ganz, P.A., Bower, J.E., Petersen, L., Abraham, L., Greendale, G.A., 2004. Neurocognitive performance in breast cancer survivors exposed to adjuvant chemotherapy and tamoxifen. J. Clin. Exp. Neuropsychol. 26, 955–969. https://doi.org/10.1080/13803390490510905.

Cella, D., Land, S.R., Chang, C.-H., Day, R., Costantino, J.P., Wolmark, N., Ganz, P.A., 2008. Symptom measurement in the Breast Cancer Prevention Trial (BCPT) (P-1): psychometric properties of a new measure of symptoms for midlife women. Breast Cancer Res. Treat. 109, 515–526. https://doi.org/10.1007/s10549-007-9682-9.

Churchill, N.W., Strother, S.C., 2013. PHYCAA+: an optimized, adaptive procedure for measuring and controlling physiological noise in BOLD fMRI. NeuroImage 82, 306–325. https://doi.org/10.1016/j.neuroimage.2013.05.102.

Churchill, Nathan W., Oder, Anita, Abdi, Hervé, Tam, Fred, Lee, Wayne, Thomas, Christopher, Ween, Jon E., Graham, Simon J., Strother, Stephen C., 2011. Optimizing preprocessing and analysis pipelines for single-subject fMRI. I. Standard temporal motion and physiological noise correction methods. Hum. Brain Mapp. 33, 609–627. https://doi.org/10.1002/hbm.21238.

Churchill, N.W., Yourganov, G., Oder, A., Tam, F., Graham, S.J., Strother, S.C., 2012. Optimizing preprocessing and analysis pipelines for single-subject fMRI: 2. Interactions with ICA, PCA, task contrast and inter-subject heterogeneity. PLoS One 7, e31147. https://doi.org/10.1371/journal.pone.0031147.

Churchill, Nathan W., Cimprich, Bernadine, Askren, Mary K., Reuter-Lorenz, Patricia A., Jung, Mi Sook, Peltier, Scott, Berman, Marc G., 2015. Scale-free brain dynamics under physical and psychological distress: pre-treatment effects in women diagnosed with breast cancer. Hum. Brain Mapp. 36, 1077–1092. https://doi.org/10.1002/hbm.22687.

Cimprich, B., Reuter-Lorenz, P., Nelson, J., Clark, P.M., Therrien, B., Normolle, D., Berman, M.G., Hayes, D.F., Noll, D.C., Peltier, S., Welsh, R.C., 2010. Prechemotherapy alterations in brain function in women with breast cancer. J. Clin. Exp. Neuropsychol. 32, 324–331. https://doi.org/10.1080/13803390903032537.

Cloutier, J., Li, T., Mišić, B., Correll, J., Berman, M.G., 2017. Brain network activity during face perception: the impact of perceptual familiarity and individual differences in childhood experience. Cereb. Cortex 27, 4326–4338. https://doi.org/10.1093/cercor/bhw232.

Dumas, J.A., Makarewicz, J., Schaubhut, G.J., Devins, R., Albert, K., Dittus, K., Newhouse, P.A., 2013. Chemotherapy altered brain functional connectivity in women with breast cancer: a pilot study. Brain Imag. Behav. 7, 524–532. https://doi.org/10.1007/s11682-013-9244-1.

Eckart, C., Young, G., 1936. The approximation of one matrix by another of lower rank. Psychometrika 1, 211–218. https://doi.org/10.1007/BF02288367.

Fawzy, F.I., Fawzy, N.W., Arndt, L.A., Pasnau, R.O., 1995. Critical review of psychosocial interventions in cancer care. Arch. Gen. Psychiatry 52, 100–113. https://doi.org/10.1001/archpsyc.1995.03950140018003.

Ferguson, R.J., McDonald, B.C., Saykin, A.J., Ahles, T.A., 2007. Brain structure and function differences in monozygotic twins: possible effects of breast cancer chemotherapy. J. Clin. Oncol. 25, 3866–3870. https://doi.org/10.1200/JCO.2007.10.8639.

Folstein, M.F., Folstein, S.E., McHugh, P.R., 1975. Mini-mental state. J. Psychiatr. Res. 12, 189–198. https://doi.org/10.1016/0022-3956(75)90026-6.

Fox, M.D., Greicius, M., 2010. Clinical applications of resting state functional connectivity. Front. Syst. Neurosci. 4. https://doi.org/10.3389/fnsys.2010.00019.

Gerton, B.K., Brown, T.T., Meyer-Lindenberg, A., Kohn, P., Holt, J.L., Olsen, R.K., Berman, K.F., 2004. Shared and distinct neurophysiological components of the digits forward and backward tasks as revealed by functional neuroimaging. Neuropsychologia 42, 1781–1787. https://doi.org/10.1016/j.neuropsychologia.2004.04.023.

Greicius, M., 2008. Resting-state functional connectivity in neuropsychiatric disorders. Curr. Opin. Neurol. 21, 424. https://doi.org/10.1097/WCO.0b013e328306f2c5.

Iordan, A.D., Cooke, K.A., Moored, K.D., Katz, B., Buschkuehl, M., Jaeggi, S.M., Jonides, J., Peltier, S.J., Polk, T.A., Reuter-Lorenz, P.A., 2018. Aging and network properties: stability over time and links with learning during working memory training. Front. Aging Neurosci. 9. https://doi.org/10.3389/fnagi.2017.00419.

Jung, M.S., Zhang, M., Askren, M.K., Berman, M.G., Peltier, S., Hayes, D.F., Therrien, B., Reuter-Lorenz, P.A., Cimprich, B., 2017. Cognitive dysfunction and symptom burden in women treated for breast cancer: a prospective behavioral and fMRI analysis. Brain Imag. Behav. 11, 86–97. https://doi.org/10.1007/s11682-016-9507-8.

Kaiser, R.H., Andrews-Hanna, J.R., Wager, T.D., Pizzagalli, D.A., 2015. Large-scale network dysfunction in major depressive disorder: a meta-analysis of resting-state functional connectivity. JAMA Psychiatry 72, 603–611. https://doi.org/10.1001/jamapsychiatry.2015.0071.

Kelly, W.E., 2004. A brief measure of general worry: the three item worry index. North Am. J. Psychology; Winter Garden 6, 219–225.

Krishnan, A., Williams, L.J., McIntosh, A.R., Abdi, H., 2011. Partial Least Squares (PLS) methods for neuroimaging: a tutorial and review. NeuroImage, Multivar. Decod. Brain Read. Vol. 56, 455–475. https://doi.org/10.1016/j.neuroimage.2010.07.034.

Kroenke, K., Strine, T.W., Spitzer, R.L., Williams, J.B.W., Berry, J.T., Mokdad, A.H., 2009. The PHQ-8 as a measure of current depression in the general population. J. Affect. Disord. 114, 163–173. https://doi.org/10.1016/j.jad.2008.06.026.

McIntosh, A.R., Lobaugh, N.J., 2004. Partial least squares analysis of neuroimaging data: applications and advances. NeuroImage, Math. Brain Imag. 23, S250–S263. https://doi.org/10.1016/j.neuroimage.2004.07.020.

Menning, S., de Ruiter, M.B., Veltman, D.J., Koppelmans, V., Kirschbaum, C., Boogerd, W., Reneman, L., Schagen, S.B., 2015. Multimodal MRI and cognitive function in patients with breast cancer prior to adjuvant treatment — the role of fatigue. NeuroImage: Clin. 7, 547–554. https://doi.org/10.1016/j.nicl.2015.02.005.

Nelson, J.K., Reuter-Lorenz, P.A., Sylvester, C.-Y.C., Jonides, J., Smith, E.E., 2003. Dissociable neural mechanisms underlying response-based and familiarity-based conflict in working memory. PNAS 100, 11171–11175. https://doi.org/10.1073/pnas.1334125100.

Reuter-Lorenz, P.A., Cimprich, B., 2013. Cognitive function and breast cancer: promise and potential insights from functional brain imaging. Breast Cancer Res. Treat. 137, 33–43. https://doi.org/10.1007/s10549-012-2266-3.

Reynolds, C.R., 1997. Forward and backward memory span should not be combined for clinical analysis. Arch. Clin. Neuropsychol. 12, 29–40. https://doi.org/10.1016/S0887-6177(96)00015-7.

Rosenberg, M.D., Finn, E.S., Scheinost, D., Papademetris, X., Shen, X., Constable, R.T., Chun, M.M., 2016. A neuromarker of sustained attention from whole-brain functional connectivity. Nat. Neurosci. 19, 165–171. https://doi.org/10.1038/nn.4179.

Schagen, S.B., Wefel, J.S., 2017. Editorial: post-traumatic stress as the primary cause for cognitive decline—not the whole Story, and perhaps no story at all. J. Natl. Cancer Inst. 109. https://doi.org/10.1093/jnci/djx091.

Smith, S.M., Nichols, T.E., Vidaurre, D., Winkler, A.M., Behrens, T.E.J., Glasser, M.F.,

Ugurbil, K., Barch, D.M., Essen, D.C.V., Miller, K.L., 2015. A positive-negative mode of population covariation links brain connectivity, demographics and behavior. Nat. Neurosci. 18, 1565–1567. https://doi.org/10.1038/nn.4125.

Spielberger Charles, D., 2010. State-Trait Anxiety Inventory. The Corsini Encyclopedia of Psychology, Major Reference Works. https://doi.org/10.1002/9780470479216.corpsy0943.

Swainston, J., Derakshan, N., 2018. Training cognitive control to reduce emotional vulnerability in breast cancer. Psycho-Oncology 27, 1780–1786. https://doi.org/10.1002/pon.4727.

Tingley, D., Yamamoto, T., Hirose, K., Keele, L., Imai, K., 2014. Mediation: R Package for Causal Mediation Analysis. (UCLA Statistics/American Statistical Association).

Tzourio-Mazoyer, N., Landeau, B., Papathanassiou, D., Crivello, F., Etard, O., Delcroix, N., Mazoyer, B., Joliot, M., 2002. Automated anatomical labeling of activations in SPM using a macroscopic anatomical parcellation of the MNI MRI single-subject brain. NeuroImage 15, 273–289. https://doi.org/10.1006/nimg.2001.0978.

Wefel, Jeffrey S., Saleeba, Angele K., Buzdar, Aman U., Meyers, Christina A., 2010. Acute and late onset cognitive dysfunction associated with chemotherapy in women with breast cancer. Cancer 116, 3348–3356. https://doi.org/10.1002/cncr.25098.

Wefel, J.S., Vardy, J., Ahles, T., Schagen, S.B., 2011. international cognition and cancer task force recommendations to harmonise studies of cognitive function in patients with cancer. Lancet Oncol. 12, 703–708. https://doi.org/10.1016/S1470-2045(10)70294-1.

Yellen, S.B., Cella, D.F., Webster, K., Blendowski, C., Kaplan, E., 1997. Measuring fatigue and other anemia-related symptoms with the Functional Assessment of Cancer Therapy (FACT) measurement system. J. Pain Symptom Manag. 13, 63–74. https://doi.org/10.1016/S0885-3924(96)00274-6.